ATA memo 21

350-antenna sample configurations for the Allen Telescope Array

Douglas Bock

Radio Astronomy Laboratory, University of California at Berkeley

March 28, 2001

ABSTRACT

This memo presents three sample configurations for the ATA. One of these consists of antennas randomly distributed across the central Hat Creek site. The others are a doughnut and a maximally filled array, for comparison purposes. The arrays are evaluated for sidelobe structure and size, antenna shadowing, sensitivity to extended structure, and connectivity cost.

1. Introduction

The ATA configuration will be unique among current instruments. Although it might be a model for a station of the Square Kilometer Array, simulations of that instrument are not yet far advanced. The large number of the randomly-distributed antennas will provide a two-dimensional[1] snapshot beam with the lowest sidelobes in all radio interferometry, and comparable with those obtained by single dish instruments. The large number (350) of antennas makes moving them impractical, so an early careful consideration of the configuration takes on a particular importance.

The simulations presented in this memo are part of a series made for discussion during evaluation of the RAL's configuration science requirements (Bock 2001). In an earlier memo (Bock 2000) I presented some similar 50-antenna configurations. The order of events has been to begin with 'fiducial' configurations which approximately fit the site, iterate with users while considering the scientific objectives, and refine the configurations while adding better site models etc. This memo describes work mid-way through the effort, using approximate site models and avoiding detailed machine optimization. Detailed site models and sophisticated optimization routines are the next step.

The land available for the ATA is shown in Figure 8. This land includes the current BIMA site and additions negotiated with the Bidwell Ranch and proposed to the US Forest Service.

---

[1] One dimensional arrays with many elements have similarly low sidelobes, but a very broad beam in the non-arrayed direction.

The intricate lava flows severely constrain possible configurations in certain regions, although it is expected that antennas can be placed on some of the land, particularly to the north of the `T`.

2. Tools for studying configurations

This business makes use of a variety of tools, some of which are summarized here for convenience. I have not yet used all of these, but intend to!

Configuration generation Configuration generation (without optimization) occurs when a configuration is designed using some rules, or manually. The following programs have been useful:

- *Virtual Radio Interferometer.* This java program was originally developed for ATCA configuration analysis and is available at `http://www.jb.man.ac.uk/~nm`. It gives real time *uv* coverages, beams, and responses to some simple source models, with adjustable hour angle and declination ranges. Rob Ackermann made some useful modifications for the version I used.
- *Mathematica.* Routines written in the mathematica language have been used to design configurations with the probability of placement governed by simple rules (such as constant, or 2-D Gaussian). Allowed regions are described by polygons obtained from the *AutoCAD* map of the observatory. Mathematica has also been used to generate geometrical patterns such as spirals.

Configuration optimization The following packages available for optimizing configurations were developed for ALMA. Each package provides a method for specifying allowed areas, although the Boone and Kogan methods are more sophisticated (reading FITS images). However, note that the configurations presented in this memo have not yet been optimized.

- *Boone* has written a package which moves antennas in order to model desired radially symmetric *uv* distributions. The package is versatile and good preliminary results have been obtained for ATA configurations. These will be presented in a future memo.
- *Kogan's* AIPS routine `CONFI` minimizes sidelobes in a region around the primary beam. I have not yet used this program.
- *Keto's* package (with Melvyn Wright's added site masking constraint) optimizes for a uniform *uv* coverage, which is probably not what we want for the ATA.

configuration	beam	
	natural	uniform
12	$73'' \times\ 66''$	$48'' \times\ 43''$
13	$74'' \times\ 70''$	$54'' \times\ 52''$
14	$150'' \times 145''$	$102'' \times 100''$

Table 1: Naturally- and uniformly-weighted beamsizes of the arrays ($\delta \times \alpha$) at $\delta = 30°$

Configuration evaluation

- *Boone's* `IDL` code plots configurations, *uv* distributions and compares them radially and azimuthally to a model.
- $\mathcal{MIRIAD}$ routines are useful since they represent the paths real data reduction takes. They are easy to script.
- `aips++` may be the way of the future, but I have not yet tried it!

3. Sample arrays

Three arrays were constructed for these simulations, using tasks written for mathematica. Antenna positions were generated randomly. To be accepted, a position had to be within the allowed regions and not closer than 11 meters[2] to any existing antenna. 350 antenna positions were generated for each array. Figure 1(a) shows a proposed array where the antennas are distributed over a central part of the Hat Creek site expected to be available for the ATA (i.e. generally outside the USFS 'inventoried roadless area'). The area available for the placement of antennas was specified by polygons describing allowed and forbidden regions. All allowed areas had equal probability of being chosen for the the placement of an antenna. Figure 1(b) shows a doughnut array of similar natural resolution whose antennas have a Gaussian distribution about a circle 250 m in diameter. Figure 1(c) is one of the most compact arrays possible with a minimum distance between antennas of 11 m.[3] The diameter of this array is 145 m. Table 1 gives the natural and uniformly-weighted beamsizes of the configurations, as determined by $\mathcal{MIRIAD}$ `invert`. The beams themselves are shown in Figure 2.

The only really good beam is that for configuration 14. This configuration has lower resolution than generally desired for the ATA. The response of configuration 12 has complicated (6%) near-in sidelobe structure, with an irregular shaped beam, but is of a desirable size. The magnitude of the

[2]This is a conservative estimate of the minimum separation required for the 6.1m ATA antennas.

[3]This is not an yet an optimally compact random array, but approaches that result. A significantly more compact array would need to take on a regularity resulting in undesired grating responses.

(a) configuration 12

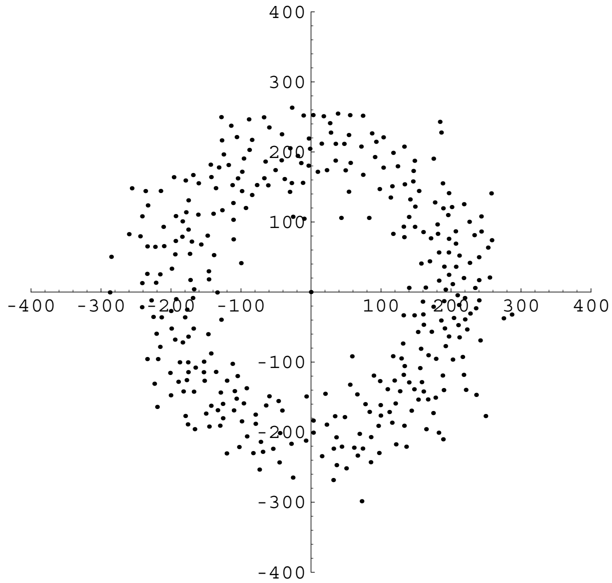

(b) configuration 13

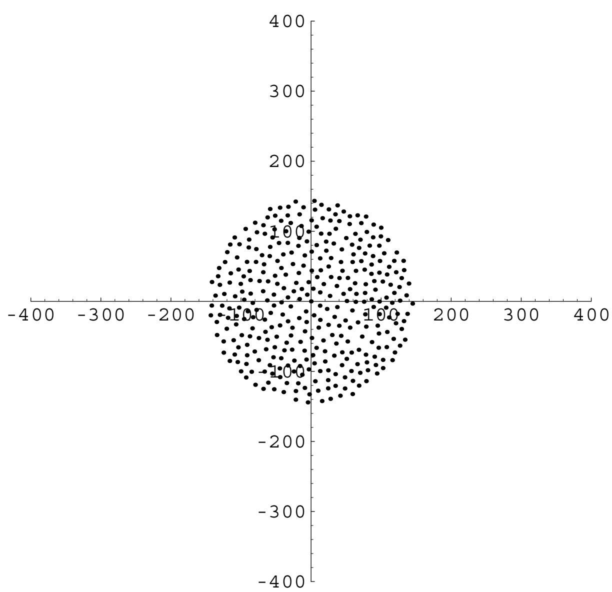

(c) configuration 14

Fig. 1.— Sample arrays, labeled in meters. Antenna sizes are to scale. The allowed and disallowed areas are shown for configuration 12. The numbering scheme is arbitrary but unique among my memos.

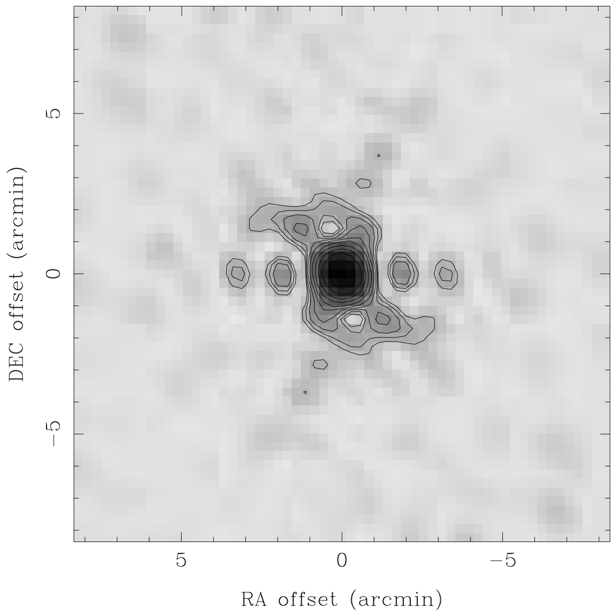

(a) configuration 12

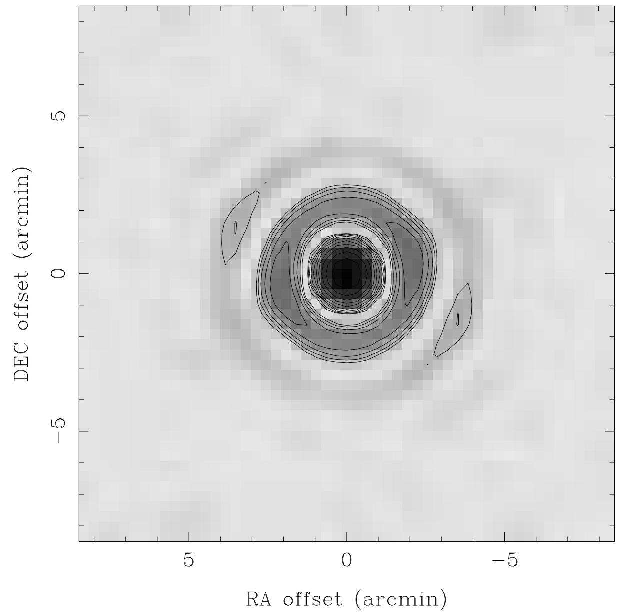

(b) configuration 13

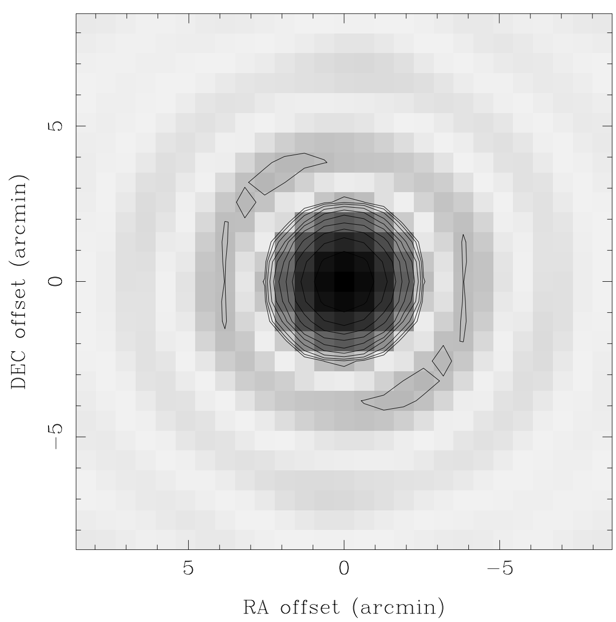

(c) configuration 14

Fig. 2.— Naturally-weighted beams for the sample arrays. The countours are logarithmically spaced, at 1.7, 2.6, 3.9, 5.9, 8.8, 13, 20, 30, 44, 67% of the peak

sidelobes is due largely to the evenness of the antennas in the site (to obtain this resolution). But the shape comes from the irregularity of the available land. It will be possible to improve the shape of the beam and reduce the size of the sidelobes by moving antennas to compensate for irregularity of the available land. But the lowest sidelobes will require a compromise on resolution.

The beam of configuration 13 is round but has a ring-like sidelobe structure that will complicate deconvolution; although it is of the same magnitude as that of configuration 12, much more power is in the near sidelobe. The tapering of the Gaussian distribution has not reduced the sidelobes sufficiently to make configurations such as this suitable candidates for the ATA, even though a slightly modified version would fit on the site reasonably conveniently.

4. Shadowing

An important concern for the design of any compact array is shadowing. An array where the antennas are evenly distributed across the available land will tend to minimize the effects, while other configurations will have higher shadowing. It is in principle possible to minimize shadowing for certain azimuth ranges. In the horizontal plane this would transfer shadowing to other azimuth ranges, and introduce a bias in the antenna distribution which might impact an array's imaging performance. By making judicious use of terrain variations one could perhaps reduce shadowing towards the south at the shortest baselines. However, this would also increase the same baselines when observing higher sources (which would not have been shadowed anyway), thus decreasing the sensitivity to extended structure at these higher elevations. It seems desirable instead to have antennas smoothly coming in and out of shadowing, while limiting the magnitude of shadowing at the lowest elevations. This also avoids potential biases in otherwise random (or optimized) configurations.

The shadowing as a function of elevation (azimuth due south) for configuration 12 is shown for several cases in Figure 3. Projects requiring the lowest sidelobes for high-fidelity imaging or RFI mitigation might use only correlations made between antennas which are not at all shadowed. However, some projects will tolerate some shadowing for increased sensitivity. The cases when 5 or 10% of an antenna may be shadowed are shown. As we can see, even the strictest constraint limits shadowing to 30% of correlations at the elevation limit of the antennas (15°). But real observations will rarely go south of the Galactic center. And the excellent snapshot imaging characteristics of the array will make repeated short tracks near transit profitable. Table 2 compares the shadowing of the three configurations during 2 hour observations (with 15-minute integrations). The transit shadowing is lower (as shown for configuration 12 in Figure 3).

The calculations above are only for observations to the south. Given the irregular site constraints, the array shadowing will vary somewhat with azimuth. Figure 4 evaluates this effect for configuration 12. This plot shows the proportion of shadowed correlations just after source rise (15°) for the range of sources available at Hat Creek. Sources with $\delta < 55°$ set below the ATA's

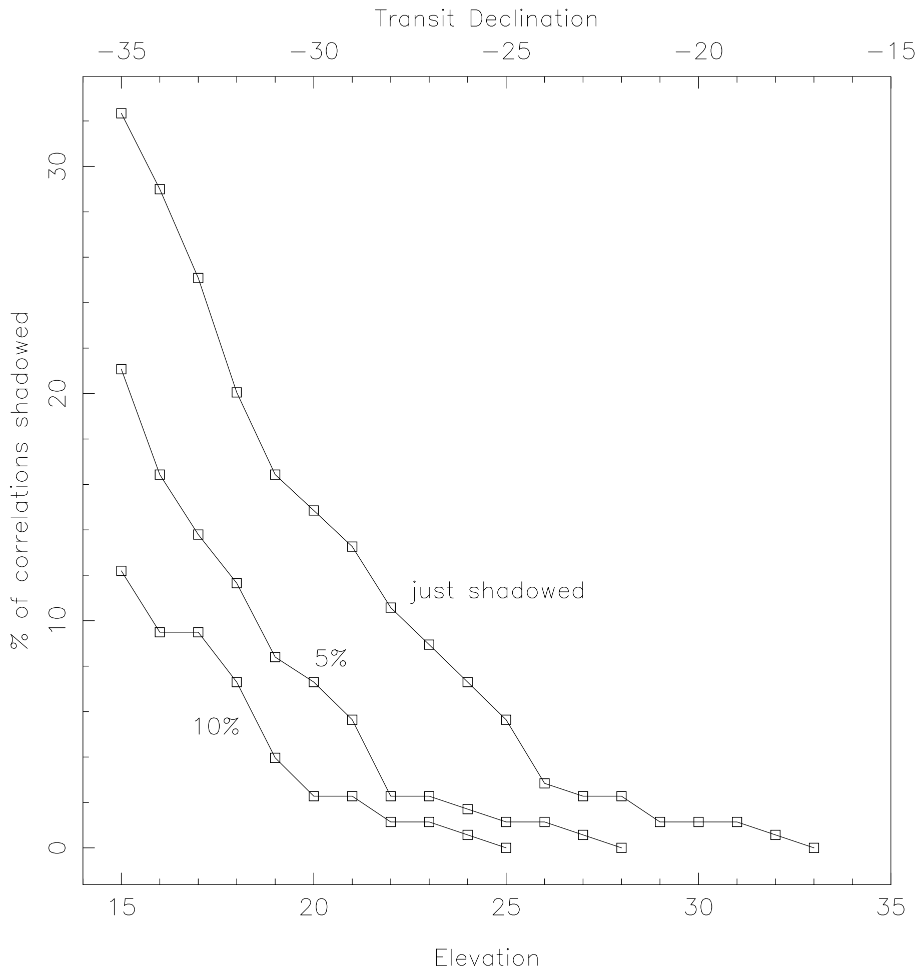

Fig. 3.— Shadowing as a function of elevation (due south) for configuration 12, with the declination of a source transiting at the specified elevation also shown. Curves are plotted for the cases of the antennas just being shadowed, and when 5% or 10% shadowing of dishes will be tolerated.

configuration	declination		
	$-30°$	$-29°$	$-20°$
12	18%	15%	2%
13	21%	18%	2%
14	61%	56%	12%

Table 2: Shadowing (percentage of correlations) for 2 hour tracks at $\delta = 30°$

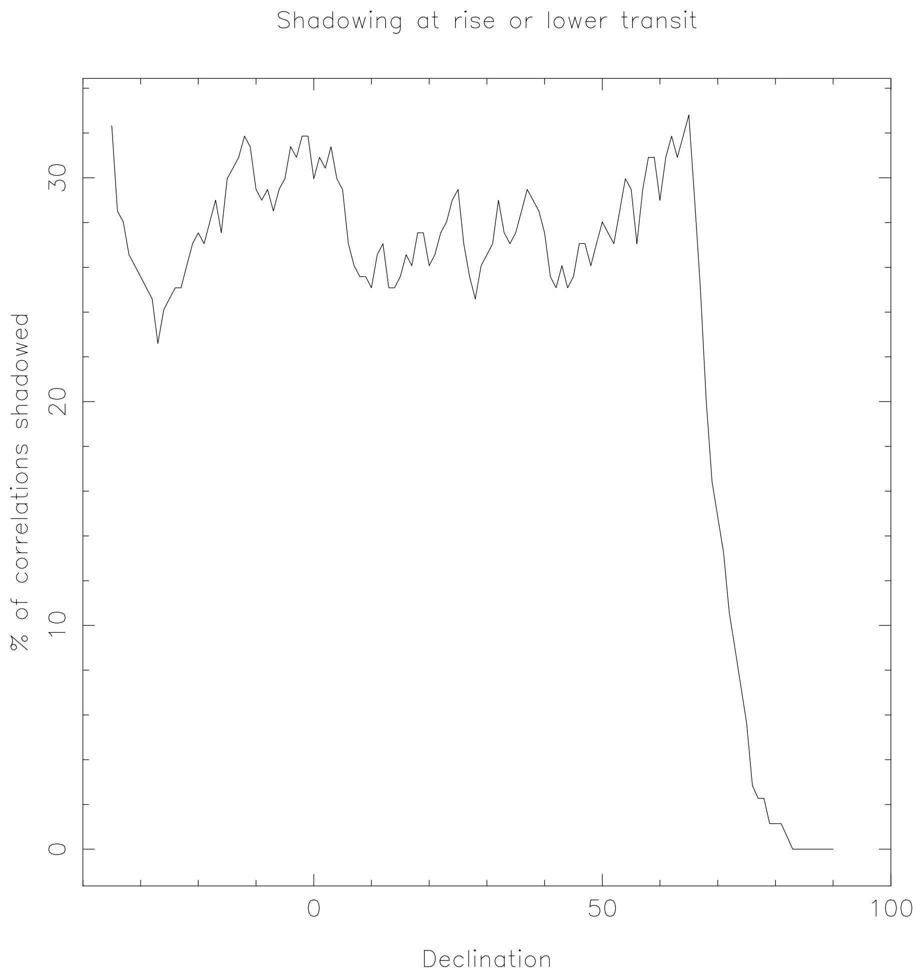

Fig. 4.— Shadowing at rise time (or lower transit for circumpolar sources) for configuration 12 as a function of declination.

elevation limit. The variation in shadowing below $\delta = 55°$ is indicative of the variation in shadowing degree with azimuth. Sources with $\delta > 55°$ are circumpolar. Observations of some of these sources will stillbe partially shadowed at their lower transit.

5. Resolution tradeoffs

What is the price of increased resolution? This section evaluates the magnitude of the 'resolving-out' problem, when the source of interest is larger than the interferometer beam.

Sensitivity as a function of scale To compare the arrays, each was used to generate a snapshot visibility distribution at $\delta = 30°$. A histogram was made of the number of visibilities as a function of angular scale. This is a measure of the collecting area, and hence sensitivity at each scale. The values of the histogram categories are plotted against angular scale in figure 5. The histogram categories are equal in width on the log scale. The benefits of the doughnut configuration are clearly seen. It has fewer intermediate spacings and more short and long spacings. This array might form the basis of a reasonable compromise between observers wanting maximum resolution and those concerned with sensitivity to structures greater than 10 arcminutes. However, its natural beamshape is poorer. The plot also makes clear the benefit of the smaller configuration to observations requiring high brightness sensitivity. The peak at the shortest spacings shows the scale sampled by many baselines at the minimum separation in such a compact configuration.

Sensitivity to physical sources The above analysis is relevant when considering specific scales, for example when trying to image or separate structures of a certain characteristic size. However, when considering simply the sensitivity to a source of a given size, it must be noted that compact spacings still detect sources which they do not resolve. Real sources are actually represented in the Fourier plane by a range of spatial frequencies. Figure 6 presents an analysis of this effect for the arrays presented above. Each point in the figure represents a simulated snapshot observation (also at $\delta = 30°$) of a Gaussian-like source of the size indicated. The actual source is a Gaussian characterized by FWHM, truncated at a diameter twice the FWHM. The truncation helps reduce the contribution of the most extended spatial components in the Gaussian. These components are undetected by almost all inteferometer pairs.

The value of each point in the figure shows the peak flux density in the dirty map, representing the degree to which the source is resolved out by the array (the peaks of well-cleaned maps are similar in value, due to the excellent uv coverage). In this analysis the doughnut array (configuration 13) generally performs slightly better than configuration 12, due its greater number of very short spacings.

It can be seen from the plots that the benefit of the doughnut configuration's extra sensitivity to the most extended structure is not overwhelming. Furthermore, its sidelobe structure (§ 3) is undesirable. The Hat Creek site could accomodate a doughnut of slightly higher resolution than presented here (it would not be very round). But the tapered outer edge would be lost, and the sidelobes would be even higher. It seems that doughnuts are not ideal for the planned ATA projects.

6. Connectivity Costs

The exact nature of the antenna connections of the ATA has yet to be resolved. The trenching costs will be in the region of 50$/m, while optical fiber can be obtained for about 3$/m. Since the RF will not be multiplexed, the cost of the RF fibers will dominate. The electricity supply and control connections can be provided much more economically. The cost of the fiber and limitations in the transmitter/receiver hardware will limit path lengths to about 1 km. The minimum trenching

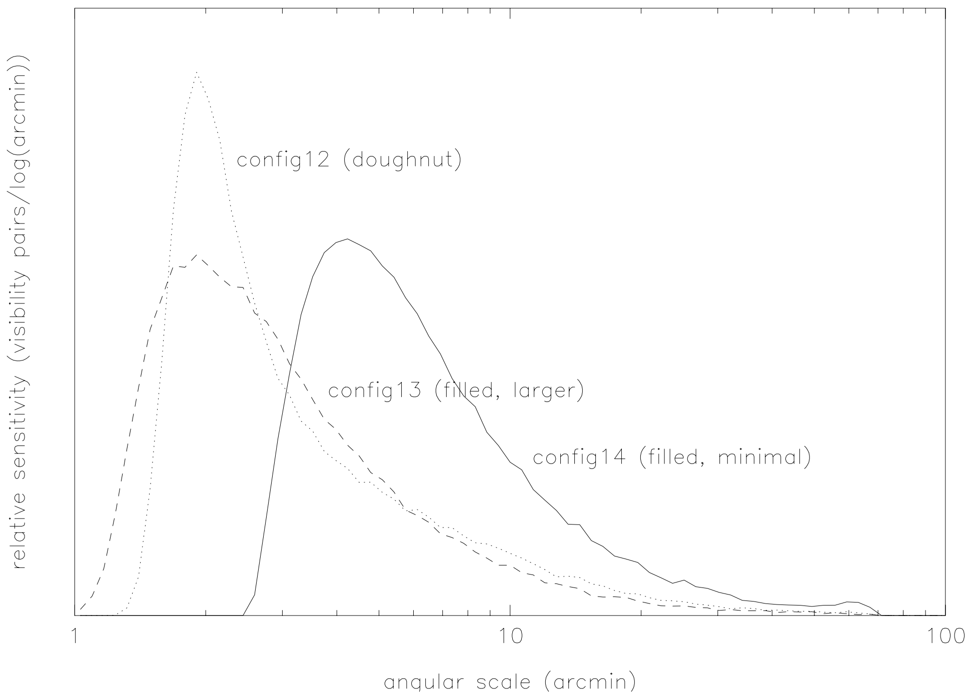

Fig. 5.— Relative sensitivity of the arrays as a function of angular scale.

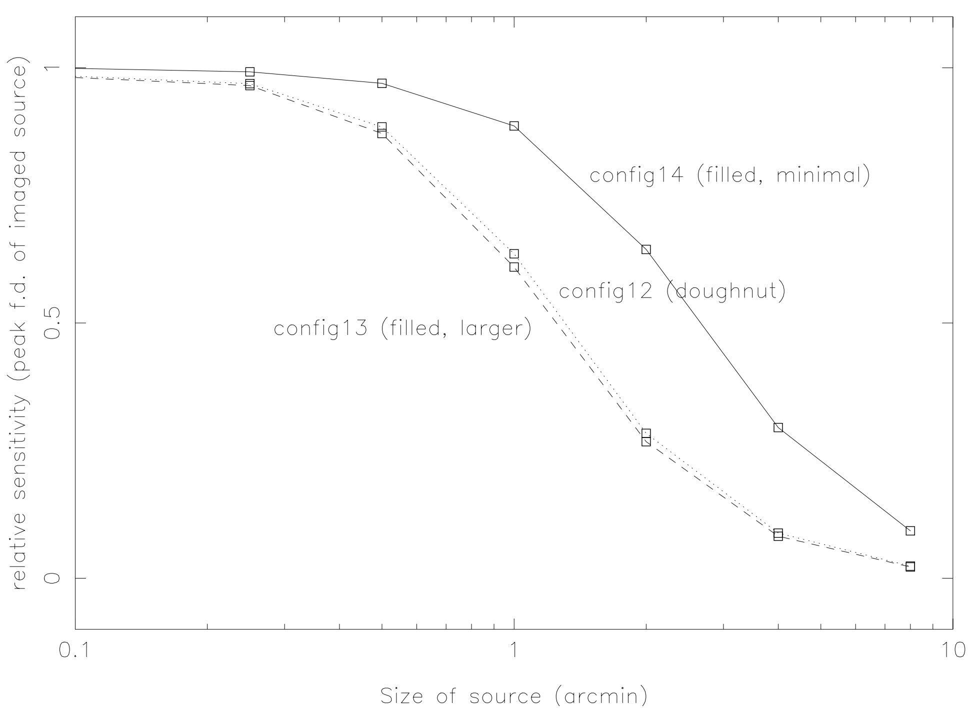

Fig. 6.— Simulated sensitivity of the arrays to a source *smaller than* a given size

costs (assuming no geographical constraints) are given by an approximate solution of the travelling salesman problem (Figure 7; Press et al. 1992). For configurations 12, 13 and 14, the approximate solutions are 8390 m, 7940 m, and 4970 m. The total length is not very sensitive to the details: all configurations under consideration have lengths of order 10 km. To keep fiber lengths below 1 km, and because the cost optimization dictates, there will be feeder trenches to the array at various points. These will probably be about 20 feeder trenches. However, are still small in total length compared to the path connecting all the antennas. So the total length of trenching will still be of order 15 km. Much more needs to be done to optimize these costs. But since they depend fundamentally on technologies, materials, and construction costs not yet fully evaluated, rather than on the exact configuration, the analysis can be deferred at present.

7. Other configurations evaluated

To gain further insight into the desirable properties of various configurations, several other possibilities were evaluated.

Northern/southern extensions The desire to image southern sources led to consideration of arrays with additional north-south extent. These fell into two classes. First, those arrays using the additional land to the far north and south of the site (Figure 8), and second, arrays where an overdensity of antennas was placed in an enlarged northern section of the array. Two adverse effects arose: the beamshape was made less symmetrical, due to the irregular shapes of land available to the north and south; and the east-west resolution was reduced since a greater proportion of the antennas were placed in the narrow regions to the north and south. It was concluded during the configuration science evaluation that the benefits did not outweigh the disadvantages of such configurations.

Effect of the trees A copse to the east of the BIMA central laboratory makes a significant hole in the land available for antenna placement. Configurations with sidelobes of order 5% (such as those in this memo) are not significantly improved by the addition of this forested area to the available land. However, this issue will need to be revisited in detail when considering future arrays better optimized for low sidelobes.

Adding the central hole As expected, forcing antennas towards the outer boundaries of the site increases the resolution of the array. It forms a distorted doughnut shape. However, the tradeoff in sidelobe levels makes this an unattractive option.

Gaussian taper Increasing the density of antennas towards the center of the available area decreases the sidelobes significantly at the expense of loss in resolution and a slight increase in shadowing. Tamara Helfer investigated this extensively in her memo on the subject (Helfer 2001).

The impact of BIMA Current plans call for the removal of BIMA to the Inyo Mountains at about the time ATA construction will begin in earnest at Hat Creek. However, should this not be the case, significant land will have to be excluded for continuing BIMA operation, especially in the central `T`. This does affect the beamshape and increase the sidelobes. Preliminary simulations show that it would be very desirable to use some of the lava to the south of the `T` under these circumstances.

In the final analysis many of the above options will be addressed by simulations which adjust antenna positions optimally for a given site. When it is clear that certain boundaries constrain antennas significantly, the boundaries in these directions will be re-examined.

8. The next step

The simulations presented in this memo were conducted to gain a basic understanding to configuration design principles as they might be applied to the ATA. The next step is to optimize for the lowest sidelobes as a function of resolution, and to choose a configuration from the sidelobe level/resolution continuum. Since connectivity costs are not very sensitive to the exact configuration, these will not drive the optimization. But they will themselves be optimized as part of the final design. Some packages are already available to do much of this work (§ 2). A detailed model of the site will need to be prepared at sub-meter resolution for this stage in the design. It will be desirable to minimize shadowing. The ATA system Preliminary Design Review committee recommended that shadowing at the Galactic center be kept to about 20–30%, and this should be born in mind for any design.

Melvyn Wright had a hand in several of the investigations described above, and joined in many stimulating discussions. Other members of the RAL and ATA project gave useful input. I am further indebted to the authors of the software described in §2.

REFERENCES

Bock, D. 2000, *50-antenna sample configurations for the Allen Telescope Array*, ATA Memo 15.

Bock, D. 2000, *Allen Telescope Array RAL Configuration Science Requirements*, ATA Memo 20.

Helfer, T. T. 2001, *Notes on Configurations for the ATA*, February 18.

Press, W. H., Teukolsky, S. A., Vetterling, W. T., and Flannery, B. P. 1992, Numerical Recipes in C (2d ed.; Cambridge: Cambridge University Press)

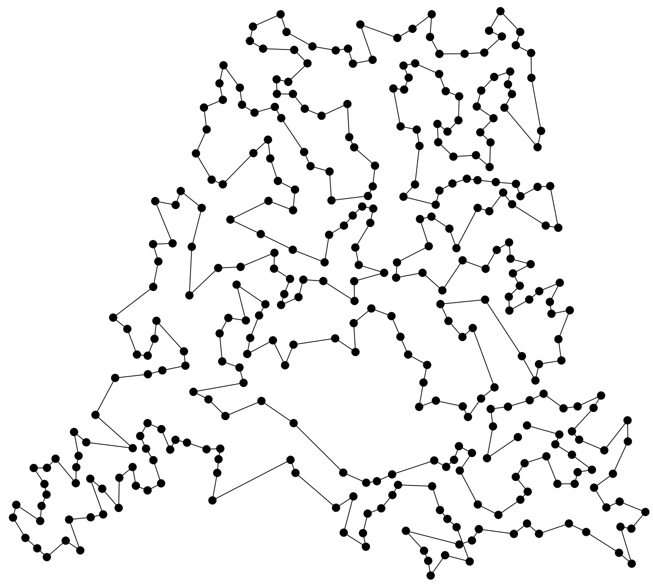

Fig. 7.— The travelling salesman problem solved (approximately) for configuration 12 (8394 m). This provides a lower bound on trenching and an upper bound on cabling costs.

Available only separately, as memo21fig8.pdf

Fig. 8.— Aerial photograph of the Hat Creek site, showing new and existing leases and use permits.